

Flames in supercritical water and their applications

PHILIPP RUDOLF VON ROHR*, KAROL PRÍKOPSKÝ,
TOBIAS ROTHENFLUH

Hydrothermal flames were firstly reported in the process of supercritical water oxidation (SCWO). The work at the ETH Zurich successfully investigated the possibility of a controlled use of hydrothermal flames to improve the process performance. Different reactor concepts were used to study continuous diffusion flames in supercritical water. In these experiments, water-methanol mixtures were used as fuel stream and oxygen as oxidizer. The ignition of the flame was achieved by heating up the reactants to auto-ignition temperatures. The concept of a transpiring-wall reactor and the hydrothermal flame as internal heat source showed a good performance in decomposition of artificial wastewater streams with salt contents up to 3 wt.%. Axial flame temperature measurements and chemiluminescence imaging were conducted to characterize the flame at various conditions in a reactor with optical access. The possibility of sustaining stable hydrothermal flames in supercritical water is a key feature for a novel drilling method.

Key words: supercritical water, SCWO, hydrothermal flames, geothermal, spallation drilling

1. Introduction

In last decades, supercritical water gained a considerable position as a reaction and process medium [1, 2]. One of the processes is the Supercritical Water Oxidation (SCWO) – a process for the disposal of toxic hazardous aqueous waste carried out at conditions above the critical point of water ($T_c = 374^\circ\text{C}$, $p_c = 22.1 \text{ MPa}$) [3]. Advantages of SCWO are high reaction rates and destruction efficiencies close to unity. The problems of corrosion and plugging of reaction vessels and components are the major challenges in the realization of the process.

In literature different approaches were studied to overcome the mentioned challenges of the process. Research groups focused on the investigations of phase behaviour of mixtures with supercritical water [4, 5], salt solubility and deposition

Transport Processes and Reaction Laboratory, Institute of Process Engineering, ETH
Zurich, Sonneggstrasse 3, 8092 Zurich, Switzerland

* Corresponding author, e-mail address: vonrorh@ipe.mavt.ethz.ch

studies [6–14], decomposition of different wastewater streams [15–21], corrosion studies [22–27] and experiments with different reactor setups [28–34].

In 1985, the research work at the University of Karlsruhe in Germany reported about the possibility of igniting flames in the environment of supercritical water [35]. First pictures and investigation results of hydrothermal flames were published shortly after [36–38]. The research on hydrothermal flames was conducted also by further research groups [39–42].

Our group focused on the investigation of hydrothermal flames in continuously operated reactors. The goal of the research was firstly, to show the feasibility of diffusion hydrothermal flames in continuous SCWO processes and secondly, to overcome the two main challenges of the process, i.e., corrosion and reactor plugging. Experiments using different reactor and burner designs, e.g., wall-cooled hydrothermal burner (WCHB) reactors, were conducted [43]. Additionally, a transpiring-wall reactor with a hydrothermal flame as internal heat source was thoroughly investigated and showed good performance in decomposition of salt-containing artificial wastewater [30, 44]. Further investigations focused exclusively on the hydrothermal flame in a novel reactor setup with optical access to understand the complex phenomena occurring during hydrothermal combustion. This work presents results of hydrothermal flame investigations and discusses the use of the flames in the field of geothermal energy mining, i.e. spallation drilling.

2. Experimental setup

In the following two reactor setups are presented, the transpiring-wall reactor and the WCHB-3 reactor.

2.1 Transpiring-wall reactor (TWR)

Figure 1 shows the concept of the transpiring-wall reactor [30]. The hydrothermal flame provides desired reaction temperatures operating at subcritical inlet temperatures, which reduces corrosion and avoids plugging (when introducing salt containing waste streams) of the reactor inlet lines. Precipitated salt is either redissolved or flushed away by the water film formed on the inner surface of the transpiring-wall.

The reactor vessel (Fig. 2) made of nickel-based Alloy 625 has an inner diameter of 34 mm and a transpiration zone length of 375 mm. The vessel was designed to sustain burst pressures up to 60 MPa and temperatures up to 600 °C. The coaxial burner setup in the upper zone of the reactor consists of a burner tube, combustion chamber and an outer insert made of Alloy 625 and separates the fuel, oxygen and wastewater inlet stream. The burner tube is an air-gap-insulated double-tube system, where the inner tube and the burner nozzle were made of Alloy 230. High-porous cylindrical elements (sintered Alloy 625 GKN Sinter Metals Filters, Radervormwald, Germany) with an inner diameter of 22 mm and a thickness of

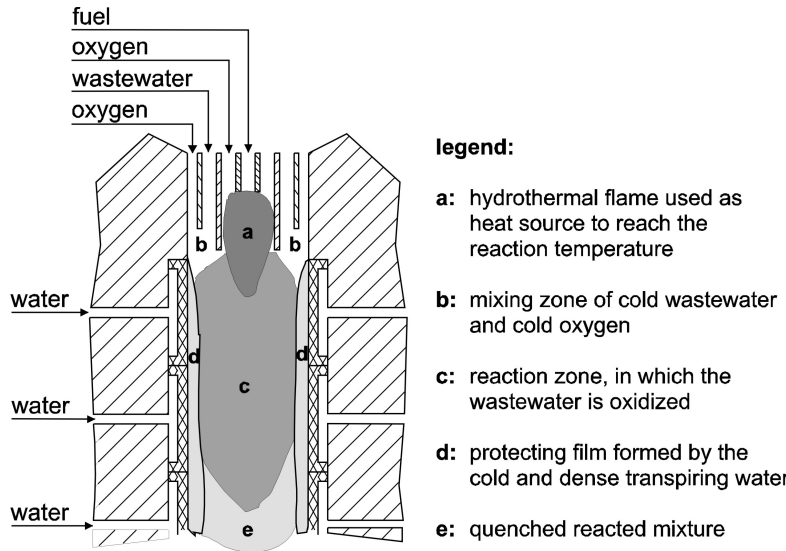


Fig. 1. Concept of the transpiring-wall reactor.

3.75 mm form the transpiring-wall. The transpiration zone has an active length of 313 mm and is divided into four separate sections. In the first three sections (TW1, TW2, TW3) the transpiring water was introduced, while in the last section (CW) cooling water was supplied. The advantage of this setup is the possibility to control the mass flow rates of the transpiring water flows and temperatures for each section separately. The elements are easy to replace and different tube porosities can be employed. We used sinter tube elements with a porosity of 17 % and 21 % in our experiments. Furthermore, three intermediate rings made of Alloy 625 allowed a lead-through of thermocouples into the transpiration zone. Four conveyor units are used for pressurizing the reactor. The system pressure is measured with a pressure transducer and controlled using a PI controller. Mass flow rates of the fuel (F_f), oxygen (F_{ox1}, F_{ox2}), wastewater (F_{ww}), transpiring ($F_{tw1}, F_{tw2}, F_{tw3}$) and cooling water (F_{cw}) flows are measured by means of Coriolis-type mass flow meters and adjusted manually. Fluid temperatures up to 600 °C are achieved using electric resistance high-pressure pre-heaters and controlled using PID controllers [30, 45].

2.2 WCHB-3 reactor

Figure 3 shows the sectional drawing of the novel wall-cooled hydrothermal burner reactor (WCHB-3). The vertical reactor vessel is made of an iron-nickel chromium Alloy A-286 and can operate pressures up to 29 MPa (burst pressure

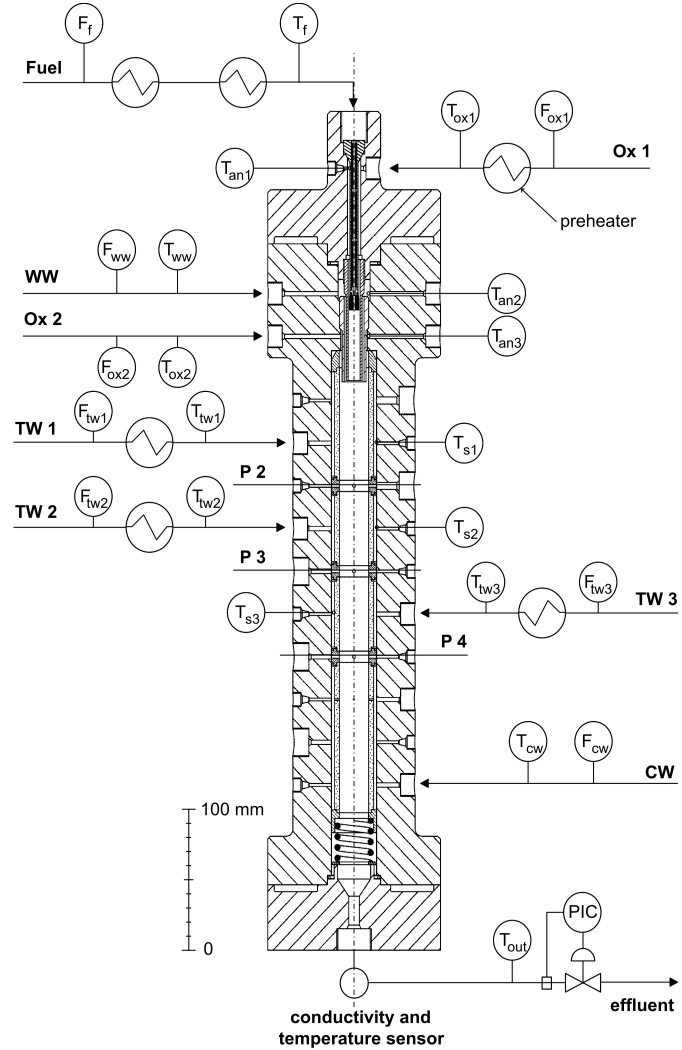


Fig. 2. Sectional drawing of the transpiring-wall reactor and pilot plant configuration. Nomenclature: F_f and T_f – mass flow rate and temperature of the fuel stream; F_{ox1} and T_{ox1} – mass flow rate and temperature of the first oxygen stream; F_{ww} and T_{ww} – mass flow rate and temperature of the wastewater stream; F_{ox2} and T_{ox2} – mass flow rate and temperature of the second oxygen stream; T_{bn} – fuel temperature in the burner nozzle (some millimetres above the tip of the burner tube), T_{an1} – Ox1 temperature in the inner annular gap, T_{an2} – WW temperature in the middle annular gap, T_{an3} – Ox2 temperature in the outer annular gap, T_{si} – TW temperature in the annular gap of section i ($i = 1, \dots, 3$), CI = on-line conductivity and temperature measurement of reactor effluent, T_{out} – temperature of reactor effluent.

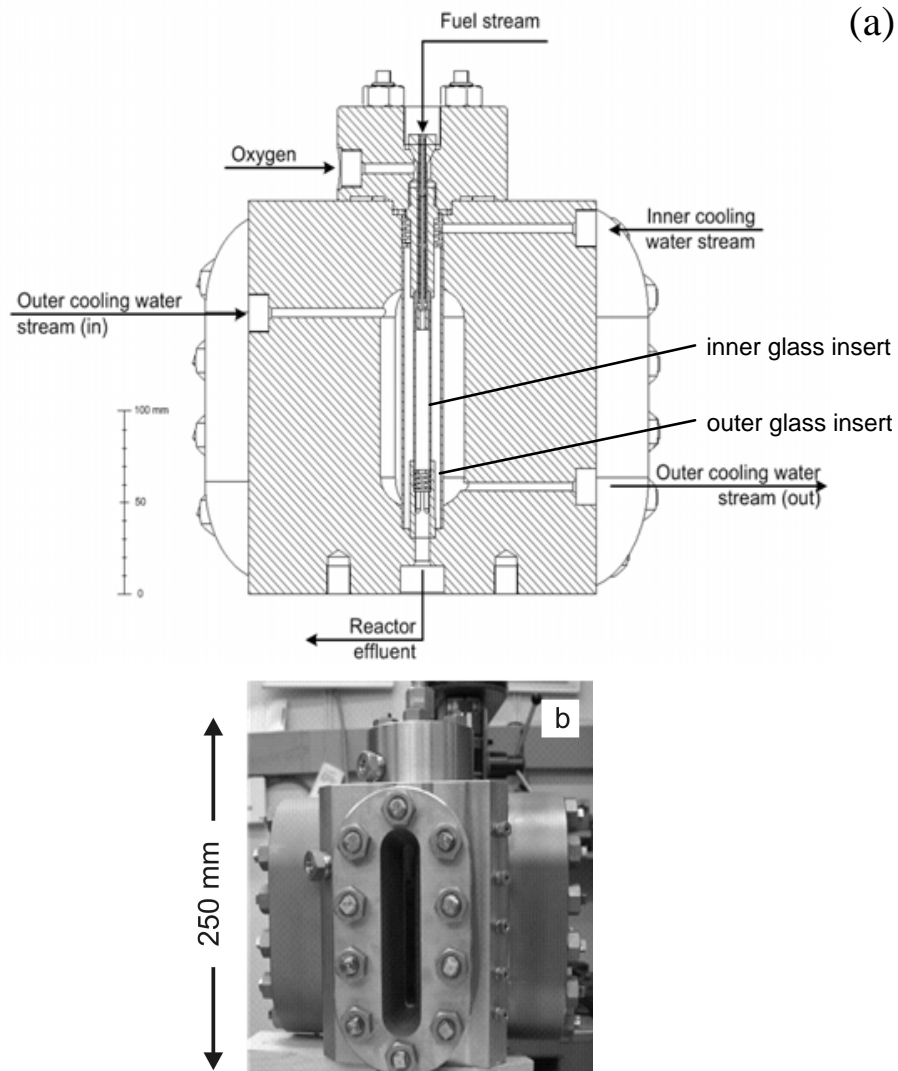


Fig. 3. Wall-Cooled Hydrothermal Burner of the third generation (WCHB-3): sectional view and picture of the manufactured reactor.

42 MPa) and temperatures up to 600 °C. The reactor design includes 4 sapphire windows which allow optical access in the full length of combustion chamber (visible length approx. 85 mm).

The combustion chamber is formed by a quartz glass cylinder with an inner and outer diameter of 8.5 mm and 10 mm, respectively. Here a methanol-water

mixture is mixing with an oxygen stream providing the hydrothermal flame combustion. The burner tube is an air-gap-insulated double-tube system, where the inner and the outer tube were made of Alloy 230. The combustion chamber is covered by the inner cooling water stream. A further quartz glass cylinder with an inner and outer diameter of 22 mm and 24 mm, respectively, separates the inner cooling water stream (CW1) from the outer cooling water stream (CW2). Thus the amount of the cooling water and the temperature in each cooling section can be controlled separately. Three conveyor units were used to pressurize the reactor. Mass flow rates of the fuel (F_f), oxygen (F_{ox}), cooling water (F_{cw1} and F_{cw2}) and fluid temperatures (T_f , T_{ox} , T_{cw1}) were adjusted with the same system as used for the TWR setup. The outer cooling water stream was not preheated.

2.3 Experimental procedure

The experimental procedure was similar for both reactor types. To achieve the ignition of the flame the fuel and oxygen stream were heated-up, until the auto-ignition temperature was reached and ignition occurred. Fuel and oxygen injection temperatures (T_f and T_{ox}) above 450 °C typically led to ignition for 12 wt.% methanol and more. After ignition, the flows and temperatures were set to desired values and kept constant. Various measurement methods were included to characterize the performance of the reactors or the hydrothermal flame, i.e. temperature and conductivity measurements, chemiluminescence imaging and analysis of effluent samples. After the completion of an experiment, fuel and salt containing flows were switched to desalinated water and temperatures were lowered step by step. The plant was cooled down 15–30 min before the pressure was reduced stepwise.

3. Results

3.1 Degradation of salt-containing artificial wastewater in the TWR

Experiments with salt-free [30] and salt-containing [44] artificial wastewater (water-methanol-sodium sulfate or water-methanol-sodium chloride) in the TWR were performed at operating pressures of 25 MPa, while oxygen was used as oxidizer. The concept using the hydrothermal flame with 16 and 22 wt.% methanol and the transpiring-wall worked satisfactory, even with sodium sulfate contents of 3 wt.% in the artificial wastewater stream. The duration of stationary conditions in the experiments lasted from 20 min up to 3 h. No plugging of the reactor was observed during the experiments. Salt residues and corrosion traces were found only in the upper/hot zone of the reactor above the protecting transpiring wall section. The salt accumulation rate was quantified using conductivity measurements with calibrated sensors and by the analysis of the reactor effluent. The use of elements of different porosity (17 and 21 %), different transpiration intensities (ratio between the mass flux of each transpiring flow and the bulk mass flux at the entrance of the

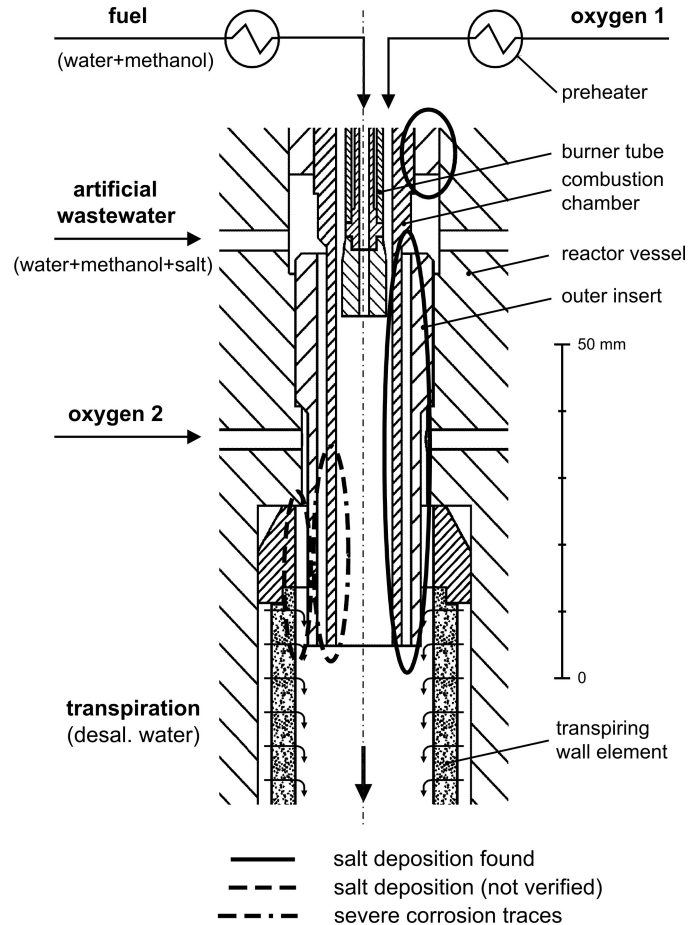


Fig. 4. Salt deposition and corrosion at the burner setup of the transpiring-wall reactor [44].

transpiring-wall tube, including the fuel, oxygen and wastewater stream; 1–6 %) and transpiring water temperatures (75–200 °C) did not significantly affect the occurring salt accumulation in the reactor. The areas of salt deposition are shown in Fig. 4.

3.2 Characterization of continuous hydrothermal diffusion flames

Further experiments focused on the characterization of continuous diffusion flames in supercritical water. For these experiments the novel WCHB-3 reactor setup with optical access was used.

As in all experiments, the ignition of the flame was achieved by heating-up the reactants (methanol-water mixtures and oxygen) to auto-ignition temperatures of 410–470 °C. Subcritical extinction temperatures were achieved with methanol mass fractions of 20 wt.% and more. Flame temperature measurements using a thermocouple and chemiluminescence of the flame were used for the characterization of the flame.

Experiments included the variation of different parameters, i.e. inlet mass flow rates, temperatures and pressure. The most significant influence on the flame had the variation of inlet temperatures and mass flow rates. The experiments mainly focused on the investigation of the hydrothermal flame combustion with supercritical injection temperatures (380–425 °C). Variation of pressure (25–27.5 MPa) and of the oxygen excess (1.2–1.6) did not show any significant influence on the flame behaviour.

The flame temperature was measured every 4 mm along the reactor axis with a time period of 10 s for each measurement point using an unshielded S-type (Platinum 10 % Rhodium (+) – pure Platinum (-)) thermocouple with a platinum sheathing. The diameter of the thermocouple was 1 mm and the response time of the thermocouple in air flow was 0.6 s (manufacturer data). The measurement allowed a rough estimation of flame temperatures and positions along the reactor axis. Figure 5 shows measured temperature profiles along the combustion chamber axis for different water-methanol mixtures. Use of higher methanol contents resulted in higher flame temperatures. However, different operating conditions adjusted in

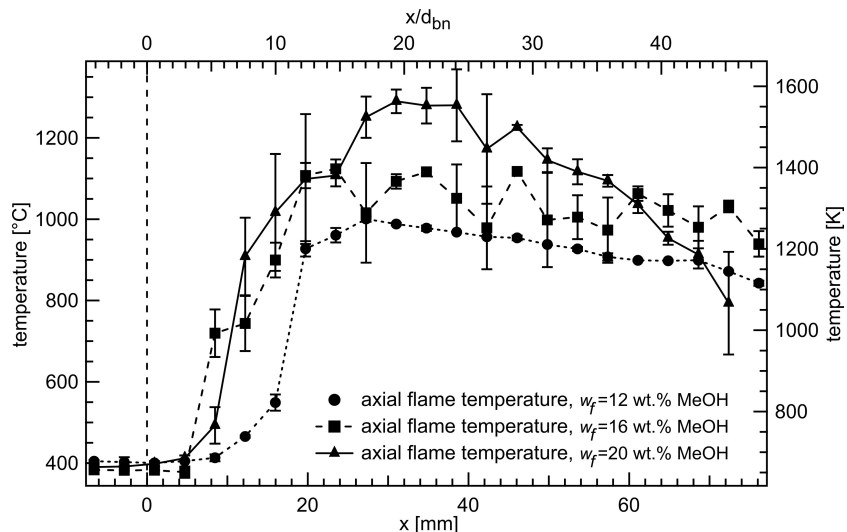


Fig. 5. Measured temperature profiles for different methanol-water mixtures.

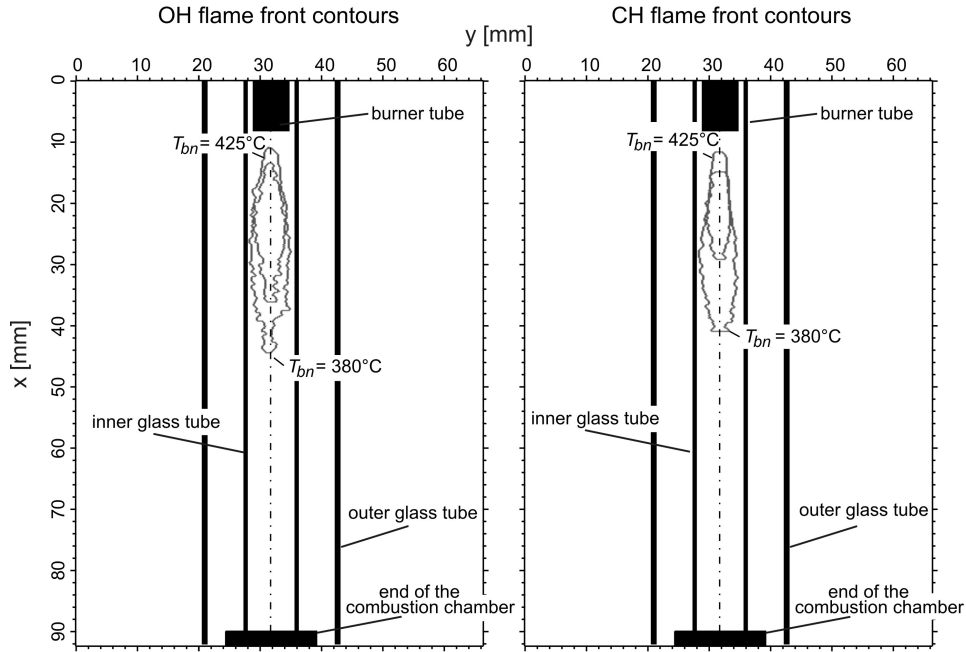


Fig. 6. Extracted flame front contours from images of OH and CH species for different fuel inlet temperatures using 16 wt.% water-methanol mixtures.

the experiments did not allow a further comparison of the results. Furthermore, the presence of the thermocouple influenced the behaviour of the flame.

CHEMILUMINESCENCE imaging was performed using an intensified CCD camera (DICAM Pro, PCO AG, Kelheim, Germany) equipped with two types of bandpass filters (313 and 431 nm). The bandpass filters were used to visualize OH and CH radicals in the flame and to gain information on the flame front position and shape. Figure 6 shows extracted flame contours from OH and CH images from experiments, where the inlet fuel temperature was varied using 16 wt.% water - methanol mixtures. With lower temperatures, the flame moved further away from the burner tube exit and became longer and broader. Due to the line-of-sight character of this method it was difficult to make conclusions on the exact position and the turbulence of the flame. However, no significant differences in flame behaviour in comparison to gaseous diffusion flames have been observed for the given supercritical conditions.

4. Conclusions and outlook

After the experiments with salt containing artificial wastewater using the TWR setup, conclusions for an improved SCWO reactor setup could be drawn.

In future transpiring-wall reactor systems the transpiring wall should cover the whole length of the reactor. In regions, where supercritical temperatures are expected, larger reactor diameters would be advantageous. As in our studies, cold wastewater should be introduced into the reactor and heat exchange surfaces and long introduction lengths in the reactor should be avoided, to minimize salt precipitation and corrosion of equipment. A direct injection of the wastewater into the flame would be desirable.

The experiments for the characterization of hydrothermal diffusion flames were a further step in understanding the complex phenomena of combustion in supercritical water environment. Once again the possibility of igniting the flame in such media could be confirmed and can also be interesting for other applications besides SCWO.

99 % of our globe is hotter than 1000 °C. Thus, geothermal energy gains more and more on importance as a sustainable energy source. Within 50 years, the USA shall produce 100 000 MW of electrical energy using this source [46]. In the same time period, Switzerland will cover approx. 750 MW of electricity production by geothermal energy use [47]. The main problems of geothermal heat mining for electricity production are a) drilling difficulties and costs, b) controlled heat exchange and c) water losses in great depths (below 5 000 m).

Spallation drilling is a possible alternative to conventional rotary drilling methods. The motivation for a new drilling method in search for oil, gas or water is the high abrasion of drilling utilities and slow approach in hard rock formations resulting in drilling costs exponentially increasing with depth. Significant cost savings are expected with spallation drilling, which makes this technology particularly interesting for geothermal energy production, where wells of great depths are needed. The idea behind this drilling method is the fast heating of a rock surface resulting in heat stresses in the rock. When the stresses become high enough, an existing flaw in the rock is extended and the surface layer breaks away from the cooler rock behind it and falls off as a thin flake also called spall (Fig. 7). Numerical simulation and testing of flame-jet spallation drilling (at ambient conditions) were presented by Rauenzahn et al. [48–50] and Wilkinson et al. [51, 52]. The hydrothermal flame could be a possible energy source for the drilling process in great depths of 2 500 m and more, where conditions similar to the SCWO process are prevailing. Water in the drill hole provides desired hydrostatic pressures and also can be used for forming fuel (H_2) and oxidation (O_2) compounds on the basis of electrolysis.

Among others, Rauenzahn and Tester [48] studied rock failure mechanisms during flame-jet spallation drilling theoretically and experimentally and proposed an equation for the rock surface temperature change at spallation.

In further studies we will focus on the heat transfer occurring between the flame and defined objects. The heat flux from a flame to objects with defined geometry, e.g. flat plates, under atmospheric conditions was investigated by several authors [53–56]. The main difference between these studies to conditions in a

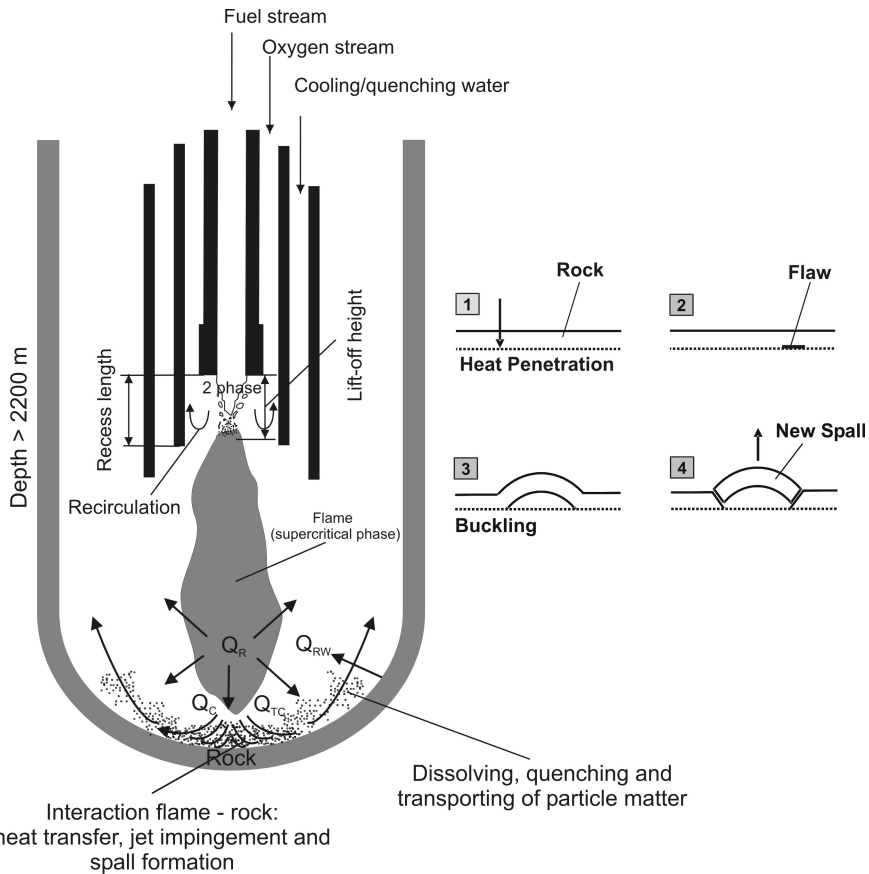


Fig. 7. Basic phenomena and their interactions occurring in the process of spallation drilling.

water-filled borehole is the lack of information about the heat transfer coefficients in supercritical water. Such studies will be performed in the above-mentioned WCHB-3 reactor. In future experiments, a flat plate equipped with heat flux sensors will be installed in the reactor allowing heat input measurements from the flame to the plate.

Acknowledgements

This work was funded by ETH Zurich and Swiss National Science Foundation (SNF).

REFERENCES

- [1] KRUSE, A.—DINJUS, E.: Journal of Supercritical Fluids, 41, 2007, p. 361.
- [2] KRUSE, A.—DINJUS, E.: Journal of Supercritical Fluids, 39, 2007, p. 362.

- [3] VERIANSYAH, B.—KIM, J. D.: *Journal of Environmental Sciences-China*, 19, 2007, p. 513.
- [4] JAPAS, M. L.—FRANCK, E. U.: *Berichte der Bunsen-Gesellschaft-Physical Chemistry Chemical Physics*, 89, 1985, p. 1268.
- [5] BRUNNER, E.: *Journal of Chemical Thermodynamics*, 22, 1990, p. 335.
- [6] BISCHOFF, J. L.—PITZER, K. S.: *American Journal of Science*, 289, 1989, p. 217.
- [7] ARMELELLINI, F. J.—TESTER, J. W.: *Journal of Supercritical Fluids*, 4, 1991, p. 2548.
- [8] ARMELELLINI, F. J.—TESTER, J. W.: *Fluid Phase Equilibria*, 84, 1993, p. 123.
- [9] ARMELELLINI, F. J.—TESTER, J. W.—HONG, G. T.: *Journal of Supercritical Fluids*, 7, 1994, p. 147.
- [10] DiPIPPO, M. M.—SAKO, K.—TESTER, J. W.: *Fluid Phase Equilibria*, 157, 1999, p. 22911.
- [11] HODES, M. et al.: *AIChE Journal*, 50, 2004, p. 2038.
- [12] HODES, M. et al.: *Journal of Supercritical Fluids*, 29, 2004, p. 265.
- [13] MARRONE, P. A. et al.: *Journal of Supercritical Fluids*, 29, 2004, p. 289.
- [14] ROGAK, S. N.—TESHIMA, P.: *AIChE Journal*, 45, 1999, p. 240.
- [15] TESTER, J. W.—WEBLEY, P. A.—HOLGATE, H. R.: *Industrial & Engineering Chemistry Research*, 32, 1993, p. 236.
- [16] COCERO, M. J. et al.: *Industrial & Engineering Chemistry Research*, 39, 2000, p. 4652.
- [17] VOGEL, F. et al.: *Journal of Supercritical Fluids*, 34, 2005, p. 249.
- [18] VERIANSYAH, B. et al.: *Journal of Hazardous Materials*, 124, 2005, p. 119.
- [19] VERIANSYAH, B.—KIM, J. D.—LEE, Y. W.: *Journal of Environmental Sciences-China*, 18, 2006, p. 13.
- [20] WILLIAMS, P. T.—ONWUDILI, J. A.: *Environmental Technology*, 27, 2006, p. 823.
- [21] VERIANSYAH, B.—KIM, J. D.—LEE, Y. W.: *Journal of Cleaner Production*, 15, 2007, p. 972.
- [22] KONYNS, J. et al.: *Corrosion*, 55, 1999, p. 45.
- [23] KRITZER, P.—BOUKIS, N.—DINJUS, E.: *Corrosion*, 56, 2000, p. 1093.
- [24] MITTON, D. B. et al.: *Industrial & Engineering Chemistry Research*, 39, 2000, p. 4689.
- [25] KRITZER, P.—DINJUS, E.: *Chemical Engineering Journal*, 83, 2001, p. 207.
- [26] MITTON, D. B. et al.: *Materials Technology*, 16, 2001, p. 44.
- [27] KRITZER, P.: *Journal of Supercritical Fluids*, 29, 2004, p. 1.
- [28] CASAL, V.—SCHMIDT, H.: *Journal of Supercritical Fluids*, 13, 1998, p. 269.
- [29] CALZAVARA, Y. et al.: *Journal of Supercritical Fluids*, 31, 2004, p. 195.
- [30] WELLIG, B.—LIEBALL, K.—RUDOLF von ROHR, P.: *Journal of Supercritical Fluids*, 34, 2005, p. 35.
- [31] BERMEJO, M. D.—COCHERO, M. J.: *Journal of Hazardous Materials*, 137, 2006, p. 965.
- [32] FAUVEL, E. et al.: *Journal of Supercritical Fluids*, 28, 2004, p. 47.
- [33] MARRONE, P. A.—CANTWELL, S. D.—DALTON, D. W.: *Industrial & Engineering Chemistry Research*, 44, 2005, p. 9030.
- [34] LEE, H. C. et al.: *Journal of Supercritical Fluids*, 36, 2005, p. 59.
- [35] FRANCK, E. U.: *Pure and Applied Chemistry*, 57, 1985, p. 1065.
- [36] FRANCK, E. U.: *Physica B & C*, 139, 1986, p. 21.
- [37] FRANCK, E. U.: *Journal of Chemical Thermodynamics*, 19, 1987, p. 225.

- [38] FRANCK, E. U.: Pure and Applied Chemistry, 59, 1987, p. 25.
- [39] STEEPER, R. R. et al.: Journal of Supercritical Fluids, 5, 1992, p. 262.
- [40] SATO, H. et al.: High Pressure Research, 20, 2001, p. 403.
- [41] SERIKAWA, R. M. et al.: Fuel, 81, 2002, p. 1147.
- [42] SOBHY, A.—BUTLER, I. S.—KOZINSKI, J. A.: Proceedings of the Combustion Institute, 31, 2007, p. 3369.
- [43] La ROCHE, H. L.—WEBER, M.—TREPP, C.: Chemical Engineering & Technology, 20, 1997, p. 208.
- [44] PRÍKOPSKÝ, K.—WELLIG, B.—RUDOLF von ROHR, P.: Journal of Supercritical Fluids, 40, 2007, p. 246.
- [45] WELLIG, B.: ETH Zurich (<http://www.e-collection.ethz.ch>). Zurich, no. 15'038, 2003.
- [46] The Future of Geothermal Energy: Impact of Enhanced Geothermal Systems (EGS) on the United States in the 21st Century. Cambridge, USA, Massachusetts Institute of Technology 2006.
- [47] Road Map Erneuerbare Energie Schweiz, SATW-Schrift, Nr. 39, Zurich, Swiss Academy for Engineering Sciences (SATW) 2006.
- [48] RAUENZAHN, R. M.—TESTER, J. W.: International Journal of Rock Mechanics and Mining Sciences & Geomechanics Abstracts, 26, 1989, p. 381.
- [49] RAUENZAHN, R. M.—TESTER, J. W.: International Journal of Heat and Mass Transfer, 34, 1991, p. 795.
- [50] RAUENZAHN, R. M.—TESTER, J. W.: International Journal of Heat and Mass Transfer, 34, 1991, p. 809.
- [51] WILKINSON, M. A.—TESTER, J. W.: International Journal of Heat and Mass Transfer, 36, 1993, p. 3459.
- [52] WILKINSON, M. A.—TESTER, J. W.: Rock Mechanics and Rock Engineering, 26, 1993, p. 29.
- [53] VISKANTA, R.: Experimental Thermal and Fluid Science, 6, 1993, p. 111.
- [54] CHANDER, S.—RAY, A.: Energy Conversion and Management, 46, 2005, p. 2803.
- [55] CHANDER, S.—RAY, A.: International Journal of Heat and Mass Transfer, 50, 2007, p. 640.
- [56] CHANDER, S.—RAY, A.: Experimental Heat Transfer, 19, 2006, p. 15.

Received: 18.12.2007

Revised: 17.4.2008